A stabilized finite element method for the two-field and three-field Stokes eigenvalue problems

Önder Türk[a,b], Daniele Boffi[c], Ramon Codina[a,*]

[a] *Universitat Politècnica de Catalunya, Barcelona, Spain*
[b] *Gebze Technical University, Gebze/Kocaeli, Turkey*
[c] *Università di Pavia, Pavia, Italy*

Abstract

In this paper, the stabilized finite element approximation of the Stokes eigenvalue problems is considered for both the two-field (displacement-pressure) and the three-field (stress-displacement-pressure) formulations. The method presented is based on a subgrid scale concept, and depends on the approximation of the unresolvable scales of the continuous solution. In general, subgrid scale techniques consist in the addition of a residual based term to the basic Galerkin formulation. The application of a standard residual based stabilization method to a linear eigenvalue problem leads to a quadratic eigenvalue problem in discrete form which is physically inconvenient. As a distinguished feature of the present study, we take the space of the unresolved subscales orthogonal to the finite element space, which promises a remedy to the above mentioned complication. In essence, we put forward that only if the orthogonal projection is used, the residual is simplified and the use of term by term stabilization is allowed. Thus, we do not need to put the whole residual in the formulation, and the linear eigenproblem form is recovered properly. We prove that the method applied is convergent, and present the error estimates for the eigenvalues and the eigenfunctions. We report several numerical tests in order to illustrate that the theoretical results are validated.

Keywords: Stokes eigenvalue problem, stabilized finite elements, two-field, three-field

*Corresponding author. Tel:+34934016486.
Email addresses: onder.turk@yandex.com (Önder Türk), daniele.boffi@unipv.it (Daniele Boffi), ramon.codina@upc.edu (Ramon Codina)

1. Introduction

The finite element approximation of eigenvalue problems has been studied extensively in recent years due to the important theoretical and practical applications. The significance of the analysis maintains its attraction, and the approximation of eigenvalue problems is still a subject of active research. In particular, there is a wide area of research on the Stokes eigenvalue problem which can be set into different frameworks, and some abstract results can be applied to a variety of mixed or hybrid type finite element eigenvalue approximation methods (see e.g. [1]).

In this paper, the problem under consideration consists of finding eigenvalues $\lambda \in \mathbb{R}$ and eigenfunctions $u \neq 0$ for a certain operator $\mathscr{L}$ on a given domain Ω such that

$$\mathscr{L}u = \lambda u \quad \text{in } \Omega, \tag{1}$$

accompanied with appropriate boundary conditions on $\partial\Omega$.

Let $\mathcal{X}$ be a Hilbert space for which the variational form of (1) is well defined. After normalizing u, this variational form reads: find a nonzero $u \in \mathcal{X}$ and $\lambda \in \mathbb{R}$ such that

$$B(u, v) = \lambda(u, v) \quad \forall v \in \mathcal{X}, \tag{2}$$

where B is the bilinear form associated to $\mathscr{L}$ and $(\cdot, \cdot)$ stands for the inner product in $L^2(\Omega)$.

Let $\mathcal{X}_h$ be a finite dimensional space of $\mathcal{X}$ constructed from a finite element partition of size h. The Galerkin discretization of (2) is: find $0 \neq u_h \in \mathcal{X}_h$ and $\lambda_h \in \mathbb{R}$ such that

$$B(u_h, v_h) = \lambda_h(u_h, v_h) \quad \forall v_h \in \mathcal{X}_h. \tag{3}$$

It is well known that when $\mathscr{L}$ is either the two-field or three-field Stokes operator, the standard Galerkin approach necessitates an interpolation for the different fields satisfying the classical inf-sup (or Babuška-Brezzi) condition. Researchers might want to avoid the use of schemes satisfying this condition. This demand has led to many recent studies devoted to develop robust and efficient stabilized techniques for approximating the Stokes eigenvalue problem [2, 3, 4, 5, 6]. It is worth noting that there are also alternative approaches. For instance, a solution procedure based on a pseudostress-velocity formulation, leading to a locally conservative scheme without using additional stabilizing terms, has been proposed in [7].

In the convergence analysis of the eigenvalue problems, the most common approach is to deduce the error estimates and the rate of convergence from the well known Babuška-Osborn theory [8] (see also [9] for a comprehensive review of finite element approximation of general eigenvalue problems). In particular, the convergence of the eigenvalues and eigenvectors for the two-field Stokes problem using mixed formulations is analyzed in many works, including [1], [9] and [10]. On the other hand, despite the extensive number of papers on finite element analysis of the eigenproblem, as well as of the source problem for the two-field Stokes operator, few works have been published on the three-field case. Considering the source problem, a stabilized finite element formulation based on a subgrid concept is presented and analyzed for the stress-displacement-pressure formulation in [11]. As another work, a Galerkin least-square based method is proposed in [12], with stability and convergence results given for the three-field Stokes formulation arising from viscoelastic models.

The aim of this paper is to analyze the stabilized finite element method for the Stokes eigenvalue problem in both two-field and three-field formulations. The stabilization method applied is based on a subgrid scale concept. In this method, the unresolvable scales of the continuous solution are approximately taken into account. In general, when a stabilization technique based on a projection $\tilde{P}$ of the residual is applied to (2), one obtains a statement of the form

$$\begin{aligned} &B(u_h, v_h) - \lambda_h(u_h, v_h) \\ &\qquad + \sum_K (\tilde{P}(-\mathscr{L}^* v_h + \lambda_h v_h), \alpha_K \tilde{P}(\mathscr{L} u_h - \lambda_h u_h))_K = 0, \end{aligned} \tag{4}$$

where $\mathscr{L}^*$ is the formal adjoint operator of $\mathscr{L}$, and α_K is a stabilization matrix (if u_h is vector valued) of numerical parameters defined within each element domain K. Here and in the following, $\sum_K$ stands for the summation over all elements of the finite element partition, and $(\cdot,\cdot)_K$ for the $L^2(K)$-inner product.

It is clear from (4) that in general the resulting system leads to a quadratic eigenvalue problem, which, apart from being much more demanding than a linear one, could introduce eigenpairs that converge to solutions which are not solutions of the original problem (2).

In this study, the unresolved subscales are assumed to be orthogonal to the finite element space, which amounts to say that $\tilde{P} = P^{\perp}$, the appropriate orthogonal projection. Apart from its novelty in the context of Stokes eigenvalue problems, this choice is essential to establish the structure of the eigenproblem in its original form. Only in this way the components u_h and v_h in the last term of (4) vanish, the

residual is simplified, and the use of term by term stabilization is allowed. We will show that this formulation is optimally convergent for an adequate choice of the algorithmic parameters on which the method depends. This will be done by applying the classical spectral approximation theory of [8] to the associated source problems in the spirit of the methodology developed in [9]. In the convergence analysis for the two-field problem, we will make use of the stability and convergence properties of the corresponding source problem, which are adapted from [13] and [14]. For the three-field eigenvalue problem, the convergence and error estimates are based on the finite element analysis of the corresponding source problem provided in [11]. This is the first finite element approximation to the three-field Stokes eigenvalue problem to the best of our knowledge.

2. Problem statements

2.1. Preliminaries

Let us introduce some notation. In the following, the space of square integrable functions in a domain ω is denoted by $L^2(\omega)$, and the space of functions having distributional derivatives of order up to an integer $m \geq 0$ belonging to $L^2(\omega)$ by $H^m(\omega)$. The space of functions in $H^1(\omega)$ vanishing on its boundary $\partial\omega$ is denoted by $H_0^1(\omega)$. The $L^2(\omega)$ inner product in ω for scalars, vectors and tensors, is denoted by $(\cdot,\cdot)_\omega$, and the norm in a Banach space $\mathcal{X}$ is denoted by $\|\cdot\|_{\mathcal{X}}$. In what follows, the domain subscript is dropped for the case $\omega = \Omega$, $\|\cdot\|$ represents the norm on $L^2(\Omega)$, and $\|\cdot\|_m$ stands for $\|\cdot\|_{H^m(\Omega)}$ for a positive or negative m. A finite element partition of the domain Ω is denoted by $\mathcal{P}_h$, and $K \in \mathcal{P}_h$ denotes an element domain. The diameter of the finite element partition is defined as $h = \max\{h_K | K \in \mathcal{P}_h\}$, where h_K is the diameter of the element domain K. For simplicity, we will assume quasi-uniform meshes. When K is a domain of an element in a partition, $\|\cdot\|_K$ and $\|\cdot\|_{m,K}$ denote $\|\cdot\|_{L^2(K)}$ and $\|\cdot\|_{H^m(K)}$, respectively. Throughout the paper, the notation $\lesssim$ is used to denote an inequality up to a constant independent of h and of the coefficients of the differential equations. All constants involved in the analysis are dimensionless.

2.2. The two-field Stokes eigenproblem

Let Ω be bounded and polyhedral. The two-field Stokes eigenvalue problem is as follows: find $[\boldsymbol{u}, p, \lambda]$, where $\boldsymbol{u} \neq \mathbf{0}$ is the displacement or velocity field, p is

the pressure, and $\lambda \in \mathbb{R}$, such that

$$\begin{cases} -\mu\Delta\boldsymbol{u} + \nabla p = \lambda\boldsymbol{u} & \text{in } \Omega, \\ \nabla \cdot \boldsymbol{u} = 0 & \text{in } \Omega, \\ \boldsymbol{u} = \boldsymbol{0} & \text{on } \partial\Omega, \end{cases} \tag{5}$$

where $\mu > 0$ is a physical parameter. The weak form of problem (5) is obtained in the functional spaces $\mathcal{V} = (H_0^1(\Omega))^d$ and $\mathcal{Q} = L^2(\Omega)/\mathbb{R}$. Setting $\mathcal{X}_{\text{I}} = \mathcal{V} \times \mathcal{Q}$, this weak form can be written as: find $[\boldsymbol{u}, p] \in \mathcal{X}_{\text{I}}$ and $\lambda \in \mathbb{R}$ such that

$$B_{\text{I}}([\boldsymbol{u}, p], [\boldsymbol{v}, q]) = \lambda(\boldsymbol{u}, \boldsymbol{v}) \quad \forall [\boldsymbol{v}, q] \in \mathcal{X}_{\text{I}}, \tag{6}$$

where

$$B_{\text{I}}([\boldsymbol{u}, p], [\boldsymbol{v}, q]) = \mu(\nabla\boldsymbol{u}, \nabla\boldsymbol{v}) - (p, \nabla \cdot \boldsymbol{v}) + (q, \nabla \cdot \boldsymbol{u}). \tag{7}$$

It is well known that the inf-sup condition holds for the continuous problem (6), and the corresponding solution operator is compact. From the spectral theory ([8]) it follows that (6) has a sequence of real eigenvalues (see also [2, 4, 15])

$$0 < \lambda_1 \leq \lambda_2 \leq \ldots \lambda_k \ldots \leq \lim_{k\to\infty} \lambda_k = \infty,$$

and corresponding eigenfunctions

$$[\boldsymbol{u}_1, p_1], [\boldsymbol{u}_2, p_2], \ldots, [\boldsymbol{u}_k, p_k], \ldots$$

which are assumed to satisfy

$$(\boldsymbol{u}_i, \boldsymbol{u}_j) = \delta_{ij}, \quad i, j = 1, 2, \ldots$$

The standard Galerkin approximation of the variational problem can be constructed on conforming finite element spaces $\mathcal{V}_h \subset \mathcal{V}$ and $\mathcal{Q}_h \subset \mathcal{Q}$. The discrete version of problem (6) is given as follows: find $[\boldsymbol{u}_h, p_h] \in \mathcal{X}_{\text{I},h} = \mathcal{V}_h \times \mathcal{Q}_h$ and $\lambda_h \in \mathbb{R}$ such that

$$B_{\text{I}}([\boldsymbol{u}_h, p_h], [\boldsymbol{v}_h, q_h]) = \lambda_h(\boldsymbol{u}_h, \boldsymbol{v}_h) \quad \forall [\boldsymbol{v}_h, q_h] \in \mathcal{X}_{\text{I},h}. \tag{8}$$

The restriction in the possible choices for the displacement and pressure spaces dictated by the inf-sup condition motivates the use of a stabilization technique to solve this problem. The stabilized finite element formulation adopted in this paper

has its roots in the variational multiscale formulation, where the continuous space $\mathcal{X}_{\rm I}$ of the problem is approximated by $\mathcal{X}_{{\rm I},h} \oplus \tilde{\mathcal{X}}_{\rm I}$, $\tilde{\mathcal{X}}_{\rm I}$ being an approximation to the complement of $\mathcal{X}_{{\rm I},h}$ in $\mathcal{X}_{\rm I}$.

In our study, we select $\tilde{\mathcal{X}}_{\rm I}$ to be approximately orthogonal to $\mathcal{X}_{{\rm I},h}$ leading to the so-called method of orthogonal subscales [13, 14, 16]. The resulting simplified stabilized method for problem (8) that we shall use reads: find $[\boldsymbol{u}_h, p_h] \in \mathcal{X}_{{\rm I},h}$ and $\lambda_h \in \mathbb{R}$ such that

$$B_{\rm IS}([\boldsymbol{u}_h, p_h], [\boldsymbol{v}_h, q_h]) = \lambda_h(\boldsymbol{u}_h, \boldsymbol{v}_h) \quad \forall [\boldsymbol{v}_h, q_h] \in \mathcal{X}_{{\rm I},h}, \tag{9}$$

where $B_{\rm IS}([\boldsymbol{u}_h, p_h], [\boldsymbol{v}_h, q_h])$ is defined as

$$\begin{aligned} B_{\rm IS}([\boldsymbol{u}_h, p_h], [\boldsymbol{v}_h, q_h]) &= B_I([\boldsymbol{u}_h, p_h], [\boldsymbol{v}_h, q_h]) \\ &\quad + \sum_K \alpha_{1K}(P^\perp(\nabla p_h), P^\perp(\nabla q_h))_K \\ &\quad + \alpha_2(P^\perp(\nabla \cdot \boldsymbol{v}_h), P^\perp(\nabla \cdot \boldsymbol{u}_h)). \end{aligned} \tag{10}$$

α_{1K} and α_2 are the stabilization parameters, which are computed as

$$\alpha_{1K} = \frac{h_K^2}{\mu} c_1, \quad \alpha_2 = c_2 \mu$$

where c_1 and c_2 are numerical constants (see [16] for more details on the method and the stabilization parameters). In the implementation of the method, a term of the form $(P^\perp(f_h), P^\perp(g_h))$ is computed as $(f_h, g_h - P(g_h))$ where the projection onto the appropriate finite element space $P(g_h)$ can either be treated implicitly or in an iterative way.

Remark 1. *Let us remark that in the design of the stabilization parameters one could take into account the eigenvalue, considering that $\lambda \boldsymbol{u}$ is a reactive-like term (see [17]). The effect of neglecting it is that the estimates to be obtained will not be uniform in terms of the magnitude of the eigenvalue, but this is the same situation encountered in any Galerkin approximation of an eigenproblem, including the inf-sup stable approximation of the Stokes problem.*

2.3. The three-field Stokes eigenproblem

The three-field Stokes eigenvalue problem is written as follows: find $[\boldsymbol{u}, p, \boldsymbol{\sigma}]$, and $\lambda \in \mathbb{R}$ such that

$$\begin{cases} -\nabla \cdot \boldsymbol{\sigma} + \nabla p = \lambda \boldsymbol{u} & \text{in } \Omega, \\ \nabla \cdot \boldsymbol{u} = 0 & \text{in } \Omega, \\ \frac{1}{2\mu}\boldsymbol{\sigma} - \nabla^S \boldsymbol{u} = \mathbf{0} & \text{in } \Omega, \\ \boldsymbol{u} = \mathbf{0} & \text{on } \partial\Omega, \end{cases} \tag{11}$$

where $\boldsymbol{u} \neq \mathbf{0}$ is the displacement field, p is the pressure, $\boldsymbol{\sigma}$ is the deviatoric component of the stress field and $\nabla^S \boldsymbol{u}$ is the symmetrical part of $\nabla \boldsymbol{u}$. To write the weak form of problem (11), in addition to the functional spaces $\mathcal{V} = (H_0^1(\Omega))^d$ and $\mathcal{Q} = L^2(\Omega)/\mathbb{R}$, we define $\mathcal{T} = (L^2(\Omega))^d_{\text{sym}}$ as the space of symmetric tensors of second order with square-integrable components. If we now let $\mathcal{X}_{\text{II}} = \mathcal{V} \times \mathcal{Q} \times \mathcal{T}$, the weak form of the problem can be stated as the follows: find $[\boldsymbol{u}, p, \boldsymbol{\sigma}] \in \mathcal{X}_{\text{II}}$ and $\lambda \in \mathbb{R}$ such that

$$B_{\text{II}}([\boldsymbol{u}, p, \boldsymbol{\sigma}], [\boldsymbol{v}, q, \boldsymbol{\tau}]) = \lambda(\boldsymbol{u}, \boldsymbol{v}) \quad \forall [\boldsymbol{v}, q, \boldsymbol{\tau}] \in \mathcal{X}_{\text{II}}, \tag{12}$$

where

$$\begin{aligned} B_{\text{II}}([\boldsymbol{u}, p, \boldsymbol{\sigma}], [\boldsymbol{v}, q, \boldsymbol{\tau}]) = (\nabla^S \boldsymbol{v}, \boldsymbol{\sigma}) - (p, \nabla \cdot \boldsymbol{v}) + (q, \nabla \cdot \boldsymbol{u}) \\ + \frac{1}{2\mu}(\boldsymbol{\sigma}, \boldsymbol{\tau}) - (\nabla^S \boldsymbol{u}, \boldsymbol{\tau}). \end{aligned} \tag{13}$$

The Galerkin finite element approximation is obtained in the usual way, by building the conforming finite element spaces $\mathcal{V}_h \subset \mathcal{V}$, $\mathcal{Q}_h \subset \mathcal{Q}$ and $\mathcal{T}_h \subset \mathcal{T}$. If we let $\mathcal{X}_{\text{II},h} = \mathcal{V}_h \times \mathcal{Q}_h \times \mathcal{T}_h$, the problem is now: find $[\boldsymbol{u}_h, p_h, \boldsymbol{\sigma}_h] \in \mathcal{X}_{\text{II},h}$ and $\lambda_h \in \mathbb{R}$ such that

$$B_{\text{II}}([\boldsymbol{u}_h, p_h, \boldsymbol{\sigma}_h], [\boldsymbol{v}_h, q_h, \boldsymbol{\tau}_h]) = \lambda(\boldsymbol{u}_h, \boldsymbol{v}_h) \quad \forall [\boldsymbol{v}_h, q_h, \boldsymbol{\tau}_h] \in \mathcal{X}_{\text{II},h}. \tag{14}$$

It is obviously seen that the bilinear form $B_{\text{II}}([\boldsymbol{u}_h, p_h, \boldsymbol{\sigma}_h], [\boldsymbol{v}_h, q_h, \boldsymbol{\tau}_h])$ is not coercive and the inf-sup condition is not satisfied unless some stringent requirements are posed on the choice of the finite element spaces. Thus, like for the two-field formulation, the purpose of the stabilization used is to avoid the use of the inf-sup conditions and, in particular, to allow equal interpolations for all the

unknowns. The same strategy as before is followed to obtain the stabilized finite element formulation, and the method becomes: find $[\boldsymbol{u}_h, p_h, \boldsymbol{\sigma}_h] \in \mathcal{X}_{\text{II},h}$ and $\lambda_h \in \mathbb{R}$ such that

$$B_{\text{IIS}}([\boldsymbol{u}_h, p_h, \boldsymbol{\sigma}_h], [\boldsymbol{v}_h, q_h, \boldsymbol{\tau}_h]) = \lambda_h(\boldsymbol{u}_h, \boldsymbol{v}_h) \quad \forall [\boldsymbol{v}_h, q_h, \boldsymbol{\tau}_h] \in \mathcal{X}_{\text{II},h}, \tag{15}$$

where $B_{\text{IIS}}([\boldsymbol{u}_h, p_h, \boldsymbol{\sigma}_h], [\boldsymbol{v}_h, q_h, \boldsymbol{\tau}_h])$ is given as

$$\begin{aligned} B_{\text{IIS}}([\boldsymbol{u}_h, p_h, \boldsymbol{\sigma}_h], [\boldsymbol{v}_h, q_h, \boldsymbol{\tau}_h]) &= B_{\text{II}}([\boldsymbol{u}_h, p_h, \boldsymbol{\sigma}_h], [\boldsymbol{v}_h, q_h, \boldsymbol{\tau}_h]) \\ &+ \alpha_3(P^{\perp}(\nabla^S \boldsymbol{v}_h), P^{\perp}(\nabla^S \boldsymbol{u}_h)) + \alpha_4(P^{\perp}(\nabla \cdot \boldsymbol{v}_h), P^{\perp}(\nabla \cdot \boldsymbol{u}_h)) \\ &+ \sum_K \alpha_{5K}(P^{\perp}(\nabla q_h - \nabla \cdot \boldsymbol{\tau}_h), P^{\perp}(\nabla p_h - \nabla \cdot \boldsymbol{\sigma}_h))_K. \end{aligned} \tag{16}$$

The stabilization parameters of this formulation are given by

$$\alpha_3 = 2\mu c_3, \quad \alpha_4 = 2\mu c_4, \quad \alpha_{5K} = \frac{h_K^2}{\mu} c_5$$

where c_3, c_4 and c_5 are numerical constants which can be taken in a wide range, as the analysis in [11] put forth. In this paper we consider that the finite element spaces are built using equal continuous interpolation, although the extension to more general spaces, and in particular of discontinuous stresses and pressures, can be done as analyzed in [11].

3. Numerical analysis of the source problems

As we have mentioned earlier, we aim to prove that the eigensolutions of the stabilized two-field and three-field Stokes problems converge to the solutions of the corresponding spectral problems by applying the classical spectral approximation theory presented in [8] to the associated source problems. To achieve this, we will present in this section the source problems for the two-field and three-field cases, and the essential stability and convergence results. At this point, let us introduce the notation for the interpolation estimates that will allow us to define the error functions of the methods. For any $v \in H^{k_v'+1}(\Omega)$, k_v being the degree of an approximating finite element space $\mathcal{W}_h$, the interpolation errors $\varepsilon_i(v)$, $i = 0, 1$, are derived from the interpolation estimates as

$$\varepsilon_i(v) = h^{k_v''+1-i} \sum_K \|v\|_{k_v''+1,K}, \tag{17}$$

with

$$\inf_{v_h \in \mathcal{W}_h} \sum_K \|v - v_h\|_{i,K} \lesssim \varepsilon_i(v), \tag{18}$$

where $k_v'' = \min(k_v, k_v')$. Here we use v to represent the unknown $\boldsymbol{u}$, $\boldsymbol{\sigma}$ or p, and k_v denotes the corresponding order of interpolation for each v. In the results given below, we will define the error functions based on these definitions.

3.1. The two-field source problem

The source Stokes problem for the two-field case can be written as: given $\boldsymbol{f} \in (L^2(\Omega))^d$, find $[\boldsymbol{u}, p] \in \mathcal{X}_{\mathrm{I}}$ such that

$$B_{\mathrm{I}}([\boldsymbol{u}, p], [\boldsymbol{v}, q]) = (\boldsymbol{f}, \boldsymbol{v}) \quad \forall [\boldsymbol{v}, q] \in \mathcal{X}_{\mathrm{I}}. \tag{19}$$

The corresponding stabilized formulation can be written as: find $[\boldsymbol{u}_h, p_h] \in \mathcal{X}_{\mathrm{I,h}}$ such that

$$B_{\mathrm{IS}}([\boldsymbol{u}_h, p_h], [\boldsymbol{v}_h, q_h]) = (\boldsymbol{f}, \boldsymbol{v}_h) \quad \forall [\boldsymbol{v}_h, q_h] \in \mathcal{X}_{\mathrm{I},h}, \tag{20}$$

where B_{IS} is defined in (10).

The stability and convergence properties of the method used in (20) are analyzed in [13] and [14], and the following theorem is a collection of immediate consequences of the results obtained therein:

Theorem 1. *The solution of (20) satisfies the stability condition*

$$\sqrt{\mu}\|\boldsymbol{u}_h\|_1 + \frac{1}{\sqrt{\mu}}\|p_h\| \lesssim \frac{1}{\sqrt{\mu}}\|\boldsymbol{f}\|_{-1}. \tag{21}$$

Moreover, if the solution of the continuous problem has enough regularity, then the solution of (20) has the following optimal order of convergence

$$\sqrt{\mu}\|\boldsymbol{u} - \boldsymbol{u}_h\|_1 + \frac{1}{\sqrt{\mu}}\|p - p_h\| \lesssim \varepsilon_{\mathrm{I}}(h), \tag{22}$$

where $\varepsilon_{\mathrm{I}}(h)$ is the interpolation error given by

$$\varepsilon_{\mathrm{I}}(h) = \sqrt{\mu}\varepsilon_1(\boldsymbol{u}) + \frac{1}{\sqrt{\mu}}\varepsilon_0(p). \tag{23}$$

□

It is important to note that as the definition of $\varepsilon_{\mathrm{I}}(h)$ suggests, the interpolation error is of order k'' in terms of h, where $k'' = \min(k''_u, k''_p + 1)$.

Now, for reasons that will become obvious in the convergence theory given in Section 4.1, we state and prove the following theorem, which asserts the L^2-error estimate for the displacement:

Theorem 2. *If the continuous problem (19) satisfies the regularity condition*

$$\sqrt{\mu}\|\boldsymbol{u}\|_2 + \frac{1}{\sqrt{\mu}}\|p\|_1 \lesssim \frac{1}{\sqrt{\mu}}\|\boldsymbol{f}\|, \tag{24}$$

then

$$\sqrt{\mu}\|\boldsymbol{u} - \boldsymbol{u}_h\| \lesssim h^2 \left(\sqrt{\mu}\|\boldsymbol{u}\|_2 + \frac{1}{\sqrt{\mu}}\|p\|_1\right). \tag{25}$$

Proof. The proof is carried out by using a duality argument. To do this, we let $[\boldsymbol{w}, \pi] \in \mathcal{X}_{\mathrm{I}}$ and consider the following adjoint problem:

$$\begin{cases} -\mu\Delta\boldsymbol{w} - \nabla\pi = \frac{\mu}{\ell^2}(\boldsymbol{u} - \boldsymbol{u}_h) & \text{in } \Omega, \\ -\nabla\cdot\boldsymbol{w} = 0 & \text{in } \Omega, \\ \boldsymbol{w} = \boldsymbol{0} & \text{on } \partial\Omega, \end{cases} \tag{26}$$

where ℓ is a characteristic length introduced to maintain the dimensional consistency of the problem. The next step is to test the first and second equations in (26) respectively with $\boldsymbol{u} - \boldsymbol{u}_h$ and $p - p_h$. Then we have

$$\begin{aligned} \frac{\mu}{\ell^2}\|\boldsymbol{u} - \boldsymbol{u}_h\|^2 &= \mu(\nabla\boldsymbol{w}, \nabla(\boldsymbol{u} - \boldsymbol{u}_h)) + (\pi, \nabla\cdot(\boldsymbol{u} - \boldsymbol{u}_h)) - (p - p_h, \nabla\cdot\boldsymbol{w}) \\ &= B_{\mathrm{I}}([\boldsymbol{u} - \boldsymbol{u}_h, p - p_h], [\boldsymbol{w}, \pi]) \\ &= B_{\mathrm{IS}}([\boldsymbol{u} - \boldsymbol{u}_h, p - p_h], [\boldsymbol{w}, \pi]) \\ &\quad - \sum_K \alpha_{1K}(P^\perp(\nabla\pi), P^\perp(\nabla(p - p_h)))_K \\ &\quad - \alpha_2 \sum_K (P^\perp(\nabla\cdot\boldsymbol{w}), P^\perp(\nabla\cdot(\boldsymbol{u} - \boldsymbol{u}_h)))_K, \end{aligned} \tag{27}$$

where we have used the definition of B_{IS}. The last term in the expression above vanishes because $\nabla\cdot\boldsymbol{w} = 0$, and thus only the first two terms on the right-hand-side of the last equality must be bounded. Now if we let $[\tilde{\boldsymbol{w}}_h, \tilde{\pi}_h]$ be the best approximation to $[\boldsymbol{w}, \pi]$ in $\mathcal{X}_{\mathrm{I},h}$, the first of these terms can be bounded using the

consistency error coming from $B_{\rm IS}([\boldsymbol{u}-\boldsymbol{u}_h, p-p_h], [\tilde{\boldsymbol{w}}_h, \tilde{\pi}_h])$ as follows. Since $[\boldsymbol{u}, p]$ is the solution of the continuous problem (19), we have

$$B_{\rm IS}([\boldsymbol{u}, p], [\tilde{\boldsymbol{w}}_h, \tilde{\pi}_h]) = (\boldsymbol{f}, \tilde{\boldsymbol{w}}_h) + \sum_K \alpha_{1K}(P^\perp(\nabla p), P^\perp(\nabla \tilde{\pi}_h))_K \\ + \alpha_2(P^\perp(\nabla \cdot \boldsymbol{u}), P^\perp(\nabla \cdot \tilde{\boldsymbol{w}}_h)). \qquad (28)$$

Making use of (20) in (28) and noting that $\nabla \cdot \boldsymbol{u} = 0$ yields

$$B_{\rm IS}([\boldsymbol{u}-\boldsymbol{u}_h, p-p_h], [\tilde{\boldsymbol{w}}_h, \tilde{\pi}_h]) \lesssim \frac{h^2}{\mu}\|\pi\|_1\|p\|_1,$$

where we have made use of the H^1-stability of the best interpolation and the expression of α_{1K}. This same bound clearly applies to the second term in the right-hand-side of (27). Regarding the stabilizing terms applied to $([\boldsymbol{u}-\boldsymbol{u}_h, p-p_h], [\boldsymbol{w}-\tilde{\boldsymbol{w}}_h, \pi-\tilde{\pi}_h])$, we have that

$$\begin{aligned}
&\sum_K \alpha_{1K}(P^\perp(p-p_h), P^\perp(\pi-\tilde{\pi}_h))_K \\
&\quad + \alpha_2(P^\perp(\nabla\cdot\boldsymbol{u} - \nabla\cdot\boldsymbol{u}_h), P^\perp(\nabla\cdot\boldsymbol{w} - \nabla\cdot\tilde{\boldsymbol{w}}_h)) \\
&\quad \lesssim \frac{h^2}{\mu}\|\pi\|_1\|p\|_1 + \mu\|\boldsymbol{u}-\boldsymbol{u}_h\|_1\|\boldsymbol{w}-\tilde{\boldsymbol{w}}_h\|_1 \\
&\quad \lesssim \frac{h^2}{\mu}\|\pi\|_1\|p\|_1 + \mu h^2\|\boldsymbol{u}\|_2\|\boldsymbol{w}\|_2.
\end{aligned}$$

On the other hand, it is easily seen that

$$\begin{aligned}
&B_{\rm I}([\boldsymbol{u}-\boldsymbol{u}_h, p-p_h], [\boldsymbol{w}-\tilde{\boldsymbol{w}}_h, \pi-\tilde{\pi}_h]) \\
&\quad \lesssim \mu\|\nabla\boldsymbol{u} - \nabla\boldsymbol{u}_h\|h\|\boldsymbol{w}\|_2 + \|p-p_h\|h\|\boldsymbol{w}\|_2 + \|\nabla\cdot\boldsymbol{u} - \nabla\cdot\boldsymbol{u}_h\|h\|\pi\|_1 \\
&\quad \lesssim h^2\mu\|\boldsymbol{u}\|_2\|\boldsymbol{w}\|_2 + h^2\|p\|_1\|\boldsymbol{w}\|_2 + h^2\|\boldsymbol{u}\|_2\|\pi\|_1.
\end{aligned}$$

Collecting the bounds just obtained and using them in (27) yields

$$\frac{\mu}{\ell^2}\|\boldsymbol{u}-\boldsymbol{u}_h\|^2 \lesssim h^2\mu\|\boldsymbol{u}\|_2\|\boldsymbol{w}\|_2 + h^2\|p\|_1\|\boldsymbol{w}\|_2 + h^2\|\boldsymbol{u}\|_2\|\pi\|_1 + \frac{h^2}{\mu}\|\pi\|_1\|p\|_1.$$

From the elliptic regularity assumption we have that

$$\|\boldsymbol{w}\|_2 \lesssim \frac{1}{\ell^2}\|\boldsymbol{u}-\boldsymbol{u}_h\|, \quad \|\pi\|_1 \lesssim \frac{\mu}{\ell^2}\|\boldsymbol{u}-\boldsymbol{u}_h\|,$$

which when used in the previous bound yields the theorem. □

3.2. The three-field source problem

The three-field Stokes source problem can be written as: given $\boldsymbol{f} \in (L^2(\Omega))^d$, seek $[\boldsymbol{u}, p, \boldsymbol{\sigma}] \in \mathcal{X}_{\text{II}}$ such that

$$B_{\text{II}}([\boldsymbol{u}, p, \boldsymbol{\sigma}], [\boldsymbol{v}, q, \boldsymbol{\tau}]) = (\boldsymbol{f}, \boldsymbol{v}) \quad \forall [\boldsymbol{v}, q, \boldsymbol{\tau}] \in \mathcal{X}_{\text{II}}, \tag{29}$$

and the stabilized formulation is: find $[\boldsymbol{u}_h, p_h, \boldsymbol{\sigma}_h] \in \mathcal{X}_{\text{II,h}}$ such that

$$B_{\text{IIS}}([\boldsymbol{u}_h, p_h, \boldsymbol{\sigma}_h], [\boldsymbol{v}_h, q_h, \boldsymbol{\tau}_h]) = (\boldsymbol{f}, \boldsymbol{v}_h) \quad \forall [\boldsymbol{v}_h, q_h, \boldsymbol{\tau}_h] \in \mathcal{X}_{\text{II},h}, \tag{30}$$

where B_{IIS} is defined in (16).

The following theorem, which is proved in [11], asserts the stability and convergence of the finite element solution:

Theorem 3. *The solution of (30) can be bounded as*

$$\sqrt{\mu}\|\boldsymbol{u}_h\|_1 + \frac{1}{\sqrt{\mu}}\|\boldsymbol{\sigma}_h\| + \frac{1}{\sqrt{\mu}}\|p_h\| \lesssim \frac{1}{\sqrt{\mu}}\|\boldsymbol{f}\|_{-1}. \tag{31}$$

Moreover, if the solution of the continuous problem has enough regularity,

$$\sqrt{\mu}\|\boldsymbol{u} - \boldsymbol{u}_h\|_1 + \frac{1}{\sqrt{\mu}}\|\boldsymbol{\sigma} - \boldsymbol{\sigma}_h\| + \frac{1}{\sqrt{\mu}}\|p - p_h\| \lesssim \varepsilon_{\text{II}}(h), \tag{32}$$

where $\varepsilon_{\text{II}}(h)$ is the interpolation error given by

$$\varepsilon_{\text{II}}(h) = \sqrt{\mu}\varepsilon_1(\boldsymbol{u}) + \frac{1}{\sqrt{\mu}}\varepsilon_0(\boldsymbol{\sigma}) + \frac{1}{\sqrt{\mu}}\varepsilon_0(p). \tag{33}$$

□

In the same way as in the previous section, the definition of $\varepsilon_{\text{II}}(h)$ states that the interpolation error is of order k'' in terms of h, where $k'' = \min(k''_u, k''_\sigma + 1, k''_p + 1)$ for this case.

To complete the convergence analysis for the three-field source problem, below we include the theorem stated and proved in [11], which provides an L^2-error estimate for the displacement:

Theorem 4. *If the continuous three-field source problem satisfies the regularity condition*

$$\sqrt{\mu}\|\boldsymbol{u}\|_2 + \frac{1}{\sqrt{\mu}}\|\boldsymbol{\sigma}\|_1 + \frac{1}{\sqrt{\mu}}\|p\|_1 \lesssim \frac{1}{\sqrt{\mu}}\|\boldsymbol{f}\|, \tag{34}$$

then

$$\sqrt{\mu}\|\boldsymbol{u} - \boldsymbol{u}_h\| \lesssim h^2 \left(\sqrt{\mu}\|\boldsymbol{u}\|_2 + \frac{1}{\sqrt{\mu}}\|\boldsymbol{\sigma}\|_1 + \frac{1}{\sqrt{\mu}}\|p\|_1 \right). \tag{35}$$

□

4. Numerical analysis of the eigenvalue problems

In this section, we aim to apply the convergence analysis to the two-field and three-field Stokes eigenproblems. Mainly, we account for the theory developed in [9], which has its roots in the abstract spectral approximation theory of Babuška-Osborn. The convergence results, and the error estimates for the displacement in suitable norms obtained in the previous section, are considered as the constitutional steps to accomplish our tasks. We will report the sufficient and necessary conditions for the convergence of eigenvalues and eigenfunctions to the continuous problems, and the approximation rates for each case.

4.1. The two-field eigenproblem

The object of this subsection is to provide, for the two-field case, the necessary and sufficient conditions for proving that the eigenvalues and eigenfunctions of (9) converge to those of (5) with no spurious solutions, and to find an estimate for the order of convergence. As already discussed, the convergence results stated in Section 3.1 will be used following the spectral approximation theory with an analogous notation to that of [9]. However, before proceeding, we want to emphasize that the Galerkin formulation of the two-field eigenproblem (5) can be set into the framework of a standard mixed eigenvalue problem of the first type according to the classification in [9] and [10] as follows: find a nontrivial $\boldsymbol{u} \in \mathcal{V}$ and $\lambda \in \mathbb{R}$ such that for some $p \in \mathcal{Q}$

$$\begin{cases} a_{\mathrm{I}}(\boldsymbol{u}, \boldsymbol{v}) + b_{\mathrm{I}}(\boldsymbol{v}, p) = \lambda(\boldsymbol{u}, \boldsymbol{v}) \quad \forall \boldsymbol{v} \in \mathcal{V}, \\ b_{\mathrm{I}}(\boldsymbol{u}, q) = 0 \quad \forall q \in \mathcal{Q}, \end{cases} \tag{36}$$

where the bilinear forms introduced are given by

$$\begin{aligned} a_{\mathrm{I}}(\boldsymbol{u}, \boldsymbol{v}) &= \mu(\nabla \boldsymbol{u}, \nabla \boldsymbol{v}), \\ b_{\mathrm{I}}(\boldsymbol{v}, q) &= (q, \nabla \cdot \boldsymbol{v}). \end{aligned}$$

If $\mathcal{V}_h \subset \mathcal{V}$ and $\mathcal{Q}_h \subset \mathcal{Q}$ are the finite element spaces to approximate the solution, the Galerkin finite element approximation can be written as: find a nontrivial $\boldsymbol{u}_h \in \mathcal{V}_h$ and $\lambda \in \mathbb{R}$ such that for some $p_h \in \mathcal{Q}_h$ there holds

$$\begin{cases} a_{\mathrm{I}}(\boldsymbol{u}_h, \boldsymbol{v}_h) + b_{\mathrm{I}}(\boldsymbol{v}_h, p_h) = \lambda(\boldsymbol{u}_h, \boldsymbol{v}_h) \quad \forall \boldsymbol{v}_h \in \mathcal{V}_h, \\ b_{\mathrm{I}}(\boldsymbol{u}_h, q_h) = 0 \quad \forall q_h \in \mathcal{Q}_h. \end{cases} \tag{37}$$

The convergence of the eigensolutions to (37) towards those of (36) is analyzed in [9].

Let us come back to our main task of analyzing the two-field eigenvalue problem. The existence and uniqueness of the solutions to (19) and (20) allows us to define the operators $T, T_h : \mathcal{X} \to \mathcal{X}$ such that for any $\boldsymbol{f} \in \mathcal{X}$, $T\boldsymbol{f} = \boldsymbol{u}$ and $T_h\boldsymbol{f} = \boldsymbol{u}_h$ are the displacement components of the solutions to (19) and (20), respectively, where $\mathcal{X}$ can be either $(H_0^1(\Omega))^d$ or $(L^2(\Omega))^d$. Now, by means of Theorem 1, we can state the convergence of the discrete operator T_h to the continuous operator T, that is to say,

$$\|T - T_h\|_{\mathcal{L}(\mathcal{X})} \to 0 \quad \text{as} \;\; h \to 0, \tag{38}$$

which is equivalent to convergence of the eigenvalues and eigenfunctions according to the theory given in [9] and [18]. In (38), $\mathcal{L}(\mathcal{X})$ denotes the space of endomorphisms in $\mathcal{X}$ and $\|\cdot\|_{\mathcal{L}(\mathcal{X})}$ its natural norm.

We next present in the following theorem the error estimates for eigenvalues of the approximate problem:

Theorem 5. *Assume that the continuous problem satisfies the regularity condition*

$$\sqrt{\mu}\|\boldsymbol{u}\|_{k''+1} + \frac{1}{\sqrt{\mu}}\|p\|_{k''} \lesssim \frac{1}{\sqrt{\mu}} h^{k''} \|\boldsymbol{f}\|_{k''-1}, \tag{39}$$

for $k'' > 0$. Then the following optimal double order of convergence holds

$$|\lambda - \lambda_h| \lesssim \frac{\mu}{\ell^2} \left(\frac{h}{\ell}\right)^{2k''}, \tag{40}$$

where ℓ is, as before, a characteristic length scale of the problem.

Proof. For $\mathcal{X} = (H_0^1(\Omega))^d$, from Theorem 1 it follows that

$$\begin{aligned}
\sqrt{\mu}\|T\boldsymbol{f} - T_h\boldsymbol{f}\|_1 &= \sqrt{\mu}\|\boldsymbol{u} - \boldsymbol{u}_h\|_1 \\
&\lesssim \varepsilon_{\mathrm{I}}(h) \\
&\lesssim \sqrt{\mu}\, h^{k''}\|\boldsymbol{u}\|_{k''+1} + \frac{1}{\sqrt{\mu}} h^{k''}\|p\|_{k''} \\
&\lesssim h^{k''} \frac{1}{\sqrt{\mu}} \|\boldsymbol{f}\|_{k''-1} \\
&\lesssim \frac{\ell^2}{\sqrt{\mu}} \left(\frac{h}{\ell}\right)^{k''} \|\boldsymbol{f}\|_1
\end{aligned}$$

where a norm embedding has been used in the last step. The proof follows from Corollary 9.8 of [9], using the definitions of $\varepsilon_{\rm I}(h)$ and k''. □

Remark 2. *The assumption (39) for $0 < k'' < 1$ suffices to prove the convergence (38) in the proof of Theorem 5. On the other hand, the stronger assumption $k'' = 1$ is needed to obtain the L^2-error estimate given by Theorem 2, which is essential to obtain the convergence result (38) if $\mathcal{X} = (L^2(\Omega))^d$ is chosen.*

Next, we make use of Corollary 9.4 of [9] to conclude that if λ is an eigenvalue of (8) with algebraic multiplicity m, and $E = E(\lambda^{-1})\mathcal{X}$ is its generalized eigenspace, where $E(\lambda)$ is the Riesz spectral projection associated with λ, and if $E_h = E_h(\lambda^{-1})\mathcal{X}$. Then

$$\hat{\delta}(E, E_h) \lesssim \sup_{\substack{\boldsymbol{u}\in E \\ \|\boldsymbol{u}\|_{\mathcal{X}}=1}} \inf_{\boldsymbol{u}_h \in E_h} \|\boldsymbol{u} - \boldsymbol{u}_h\|_{\mathcal{X}}.$$

Having arrived at these results, one can now prove the following:

Theorem 6. *Let $\boldsymbol{u}$ be a unit eigenfunction solution of (6) associated to the eigenvalue λ of multiplicity m, and let $\boldsymbol{\phi}_h^1, \ldots, \boldsymbol{\phi}_h^m$ be the eigenfunctions associated with the m discrete eigenvalues solution of (9) converging to λ. Then there exists a discrete eigenfunction $\boldsymbol{u}_h \in \text{span}\{\boldsymbol{\phi}_h^1, \ldots, \boldsymbol{\phi}_h^m\}$ such that*

$$\|\boldsymbol{u} - \boldsymbol{u}_h\|_1 \lesssim h^{k''} \|\boldsymbol{u}\|_{k''+1}. \tag{41}$$

4.2. The three-field eigenproblem

We first remark that it is possible to obtain a standard mixed formulation for the three-field eigenproblem (11) as follows (see also [19]): find $\boldsymbol{u} \in \mathcal{V}$ and $\lambda \in \mathbb{R}$ such that for some $[\boldsymbol{\sigma}, p] \in \mathcal{T} \times \mathcal{Q}$ there holds

$$\begin{cases} a_{\rm II}([\boldsymbol{\sigma}, p], [\boldsymbol{\tau}, q]) + b_{\rm II}([\boldsymbol{\tau}, q], \boldsymbol{u}) = 0 \quad \forall [\boldsymbol{\tau}, q] \in \mathcal{T} \times \mathcal{Q}, \\ b_{\rm II}([\boldsymbol{\sigma}, p], \boldsymbol{v}) = -\lambda(\boldsymbol{u}, \boldsymbol{v}) \quad \forall \boldsymbol{v} \in \mathcal{V}, \end{cases} \tag{42}$$

where we have introduced the following bilinear forms:

$$a_{\rm II}([\boldsymbol{\sigma}, p], [\boldsymbol{\tau}, q]) = \frac{1}{2\mu}(\boldsymbol{\sigma}, \boldsymbol{\tau}),$$
$$b_{\rm II}([\boldsymbol{\sigma}, p], \boldsymbol{v}) = -(\boldsymbol{\tau} - q\boldsymbol{I}, \nabla^S \boldsymbol{u}).$$

As before, once the finite element spaces $\mathcal{V}_h \subset \mathcal{V}$, $\mathcal{Q}_h \subset \mathcal{Q}$ and $\mathcal{T}_h \subset \mathcal{T}$ have been constructed, the discrete eigenvalue problem can be written as follows: find $\boldsymbol{u}_h \in \mathcal{V}_h$ and $\lambda \in \mathbb{R}$ such that for some $[\boldsymbol{\sigma}_h, p_h] \in \mathcal{T}_h \times \mathcal{Q}_h$ there holds

$$\begin{cases} a_{\mathrm{II}}([\boldsymbol{\sigma}_h, p_h], [\boldsymbol{\tau}_h, q_h]) + b_{\mathrm{II}}([\boldsymbol{\tau}_h, q_h], \boldsymbol{u}_h) = 0 \quad \forall [\boldsymbol{\tau}_h, q_h] \in \mathcal{T}_h \times \mathcal{Q}_h, \\ b_{\mathrm{II}}([\boldsymbol{\sigma}_h, p_h], \boldsymbol{v}_h) = -\lambda_h (\boldsymbol{u}_h, \boldsymbol{v}_h) \quad \forall \boldsymbol{v}_h \in \mathcal{V}_h. \end{cases} \tag{43}$$

This is a standard mixed eigenvalue problem of the second type according to the classification in [9], and can be analyzed by using the abstract theory given there.

Our ultimate purpose in this section is to provide the necessary and sufficient conditions for proving that the eigenvalues and eigenfunctions of (15) converge to those of (12) with no spurious solutions, and to estimate the order of convergence. Thus, we now proceed to establish the convergence results based on Section 3.2, as before following the notation and the ingredients of [9]. From the well posedness of problems (29) and (30), for any $\boldsymbol{f} \in \mathcal{X}$, we can define the operators $Z, Z_h : \mathcal{X} \to \mathcal{X}$ such that $Z\boldsymbol{f} = \boldsymbol{u}$ and $Z_h \boldsymbol{f} = \boldsymbol{u}_h$ are the displacement components of the solutions to (29) and (30), respectively. In this way, Theorem 3 allows us to state the convergence

$$\|Z - Z_h\|_{\mathcal{L}(\mathcal{X})} \to 0 \quad \text{as} \ \ h \to 0, \tag{44}$$

which is equivalent to the convergence of eigenvalues and eigenfunctions we are seeking.

The following theorem provides the rate of convergence of the eigenvalues:

Theorem 7. *Assume that the continuous problem satisfies the regularity condition*

$$\sqrt{\mu}\|\boldsymbol{u}\|_{k''+1} + \frac{1}{\sqrt{\mu}}\|p\|_{k''} + \frac{1}{\sqrt{\mu}}\|\boldsymbol{\sigma}\|_{k''} \lesssim \frac{1}{\sqrt{\mu}} h^{k''} \|\boldsymbol{f}\|_{k''-1}, \tag{45}$$

for $k'' > 0$. Then have the following optimal double order of convergence

$$|\lambda - \lambda_h| \lesssim \frac{\mu}{\ell^2} \left(\frac{h}{\ell}\right)^{2k''}. \tag{46}$$

Proof. Let $\mathcal{X} = (H_0^1(\Omega))^d$. From Theorem 3 we have

$$\begin{aligned}\sqrt{\mu}\|Z\boldsymbol{f} - Z_h\boldsymbol{f}\|_1 &= \sqrt{\mu}\|\boldsymbol{u} - \boldsymbol{u}_h\|_1 \\ &\lesssim \varepsilon_{\mathrm{II}}(h) \\ &\lesssim \sqrt{\mu}h^{k''}\|\boldsymbol{u}\|_{k''+1} + \frac{1}{\sqrt{\mu}}h^{k''}\|\boldsymbol{\sigma}\|_{k''} + \frac{1}{\sqrt{\mu}}h^{k''}\|p\|_{k''} \\ &\lesssim h^{k''}\frac{1}{\sqrt{\mu}}\|\boldsymbol{f}\|_{k''-1} \\ &\lesssim \frac{\ell^2}{\sqrt{\mu}}\left(\frac{h}{\ell}\right)^{k''}\|\boldsymbol{f}\|_1.\end{aligned}$$

The proof is completed by following Corollary 9.8 of [9], and observing the definitions of $\varepsilon_{\mathrm{II}}(h)$ and k''. □

Remark 3. *The convergence for the choice of $\mathcal{X} = (L^2(\Omega))^d$ can similarly be obtained as a result of the L^2-error estimate of the displacement given in Theorem 4 by assuming that the elliptic regularity condition holds with $k'' = 1$.*

Next, we make use of Corollary 9.4 of [9] to conclude that if λ is an eigenvalue of (12) with algebraic multiplicity m, $E = E(\lambda^{-1})\mathcal{X}$ is its generalized eigenspace, where $E(\lambda)$ is the Riesz spectral projection associated with λ, and if $E_h = E_h(\lambda^{-1})\mathcal{X}$, then

$$\hat{\delta}(E, E_h) \lesssim \sup_{\substack{\boldsymbol{u}\in E \\ \|\boldsymbol{u}\|_{\mathcal{X}}=1}} \inf_{\boldsymbol{u}_h \in E_h} \|\boldsymbol{u} - \boldsymbol{u}_h\|_{\mathcal{X}}.$$

From these results we can conclude exactly the same as in Theorem 6:

Theorem 8. *Let $\boldsymbol{u}$ be a unit eigenfunction solution of (12) associated to the eigenvalue λ of multiplicity m, and let $\boldsymbol{\phi}_h^1, \ldots, \boldsymbol{\phi}_h^m$ be the eigenfunctions associated with the m discrete eigenvalues solution of (15) converging to λ. Then there exists a discrete eigenfunction $\boldsymbol{u}_h \in \mathrm{span}\{\boldsymbol{\phi}_h^1, \ldots, \boldsymbol{\phi}_h^m\}$ such that*

$$\|\boldsymbol{u} - \boldsymbol{u}_h\|_1 \lesssim h^{k''}\|\boldsymbol{u}\|_{k''+1}. \tag{47}$$

5. Numerical results

In this section we present some numerical tests to illustrate the theoretical convergence results obtained for the two-field and three-field Stokes problems in

two dimensions. Three different problem domains, namely, a square domain, an L-shaped domain, and a square with a crack, are considered in Sections 5.1, 5.2, and 5.3, respectively. The orthogonal subscale stabilization method is applied with equal order of P_1 (linear) and P_2 (quadratic) interpolations for all the unknowns on triangular elements.

It is important to note that all the theory about stabilized finite element methods applies for some fixed values of the constants defined in these parameters. The accuracy of the approximation for a fixed mesh size depends on the discretization type of the region as well as on the choice of the algebraic constants in the stabilization parameters.

In the present study, the method given in (9) is applied using fixed values of the constants, that we have chosen as $c_1 = 1/4$ and $c_2 = 1/10$ for both P_1 and P_2 elements to solve the two-field eigenproblem (5). For the three-field Stokes eigenvalue problem (11), we employ the method given in (15), where the constants of the stabilization parameters are now taken as $c_3 = 1$, $c_4 = 1/10$ and $c_5 = 1/4$.

The case $\mu = 1$ is considered for all the tests we examine, and as the exact solutions to the considered eigenproblems are unknown, reference values are taken from the works published for validation purposes. The reference values are given individually for each test case. We examine the convergence rates for the reference eigenvalue approximations in terms of the difference between the approximate value and the reference value, normalized by the latter. For each test case, we illustrate the results on a log-log scaled plane.

In the simulations, the displacement (or velocity) components are taken as zero on the whole boundary, whereas the pressure is specified to be zero at a single point of the computational domain. The computations are carried out by a code written by us using MATLAB, where the generalized eigenvalue function *eigs*, which uses ARPACK, is involved. The number of divisions in each direction is denoted by N. For the L-shaped domain, N is the number of division in one of the shortest edges.

5.1. Test 1: Square domain

In this test, we consider a widely used experiment, and solve the eigenproblems on the square $\Omega = [0, 1] \times [0, 1]$. A sample discretization of the problem domain using $N = 5$ is illustrated in Figure 1. As we have already mentioned, the exact solution is unknown, and we take $\lambda_1 = 52.3447$ as a reference to the minimum eigenvalue (see [2, 4, 20]).

Figures 2 and 3 present the convergence of the minimum eigenvalue approximations to the reference value λ_1 for the two-field and three-field problems, re-

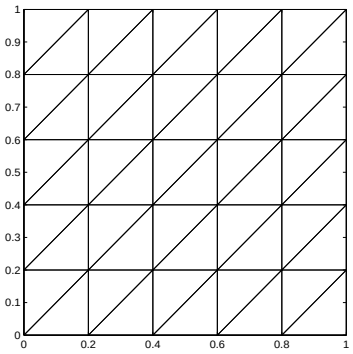

Figure 1: A sample triangulation of the square domain ($N = 5$).

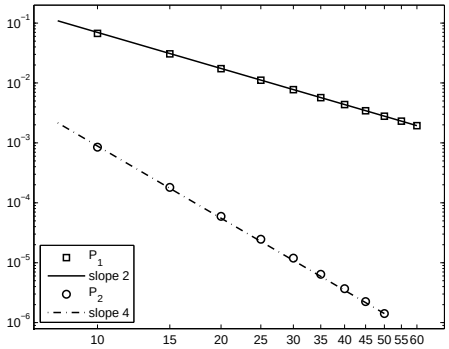

Figure 2: Plot of $\log|(\lambda_1 - \lambda_h)/\lambda_1|$ with respect to $\log|N|$for the two-field Stokes problem on a square domain.

spectively. From the two figures, we can observe the optimal convergence rates, which are 2 for P_1 elements and 4 for P_2 elements for both approximations. These calculations prove numerically that the theoretical convergence results are achieved. To have a closer glance at the computed eigenvalues, the approximation to the first eigenvalue as well as the error values are listed in Tables 1-3 (using P_1 elements) and Tables 2-4 (using P_2 elements). It can be seen from these tables that both for the P_1 and P_2 solutions, as the number of divisions (N) increases, and thus as h tends to zero accordingly, the computed eigenvalues converge to the reference value. Moreover, the results show a monotonic convergence of the approximations from above.

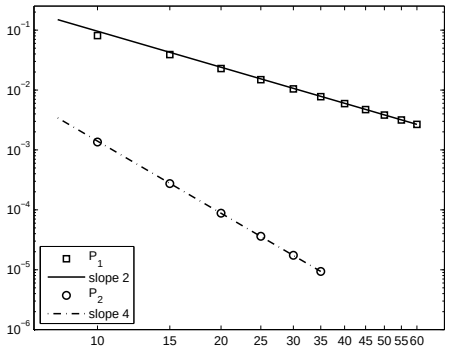

Figure 3: Plot of $\log|(\lambda_1 - \lambda_h)/\lambda_1|$ with respect to $\log|N|$ for the three-field Stokes problem on a square domain.

Table 1: Computed eigenvalues of two-field Stokes problem on a square domain using P_1 elements.

N	λ_h	$(\lambda_1 - \lambda_h)/\lambda_1$
10	55.8688	0.0673
15	53.9453	0.0306
20	53.2514	0.0173
25	52.9270	0.0111
30	52.7498	0.0077
35	52.6426	0.0057
40	52.5729	0.0044
45	52.5251	0.0034
50	52.4908	0.0028
55	52.4655	0.0023
60	52.4462	0.0019

Furthermore, we want to look at the first ten eigenvalue approximations with comparison to the reference values obtained by the standard Galerkin method using P_2-P_1 interpolations satisfying the appropriate inf-sup condition on a fine mesh ($N = 60$). The results are shown in Table 5 and Table 6 using respectively P_1 elements and P_2 elements for the two-field case. The results for the three-field case are shown in Table 7 (using P_1 elements) and Table 8 (using P_2 elements).

Table 2: Computed eigenvalues of two-field Stokes problem on square domain using P_2 elements.

N	λ_h	$(\lambda_1 - \lambda_h)/\lambda_1$
10	52.389177613831528	8.4971×10^{-4}
15	52.354184532067258	1.8119×10^{-4}
20	52.347805305859254	5.9324×10^{-5}
25	52.345990378868223	2.4652×10^{-5}
30	52.345324052984957	1.1922×10^{-5}
35	52.345034782505891	6.3957×10^{-6}
40	52.344893303689837	3.6929×10^{-6}
45	52.344817643340264	2.2475×10^{-6}
50	52.344774270297329	1.4189×10^{-6}

Table 3: Computed eigenvalues of three-field Stokes problem on square domain using P_1 elements.

N	λ_h	$(\lambda_1 - \lambda_h)/\lambda_1$
10	56.5919	0.0811
15	54.3902	0.0391
20	53.5378	0.0228
25	53.1231	0.0149
30	52.8913	0.0104
35	52.7491	0.0077
40	52.6558	0.0059
45	52.5913	0.0047
50	52.5449	0.0038
55	52.5104	0.0032
60	52.4841	0.0027

The numerical results show that the approximations for all the first ten eigenvalues in the calculated spectrum converge to the corresponding reference solutions, and the approximated values are above the reference solutions for all cases.

In order to compare our results qualitatively, we plot the unknowns, when

Table 4: Computed eigenvalues of three-field Stokes problem on square domain using P_2 elements.

N	λ_h	$(\lambda_1 - \lambda_h)/\lambda_1$
10	52.415573819924084	1.3540×10^{-3}
15	52.359070017800590	2.7453×10^{-4}
20	52.349305192050018	8.7978×10^{-5}
25	52.346595128313346	3.6205×10^{-5}
30	52.345613136524591	1.7445×10^{-5}
35	52.345190028331487	9.3616×10^{-6}

Table 5: Computed ten eigenvalues of two-field Stokes problem on a square domain using P_1 elements.

Ref.	$N = 10$	$N = 15$	$N = 20$	$N = 25$	$N = 30$	$N = 35$	$N = 40$
52.3447	55.8688	53.9453	53.2514	52.927	52.7498	52.6426	52.5729
92.1245	99.9955	95.7656	94.1952	93.4560	93.0514	92.8065	92.6471
92.1246	104.6259	97.7599	95.3019	94.1591	93.5375	93.1626	92.9192
128.2100	148.7460	138.2263	133.9922	131.9494	130.8203	130.1333	129.6851
154.1260	179.5074	165.7321	160.7009	158.3444	157.0584	156.2813	155.7763
167.0298	196.3993	179.8558	174.1717	171.5767	170.1783	169.3389	168.7957
189.5729	221.5153	205.7600	199.0557	195.7457	193.8967	192.7654	192.0246
189.5735	240.9553	214.2593	203.7305	198.6940	195.9248	194.2460	193.1532
246.3240	303.4553	271.6308	260.4574	255.3276	252.5584	250.8957	249.8195
246.3243	304.9802	275.3703	262.4826	256.6058	253.4404	251.5414	250.3128

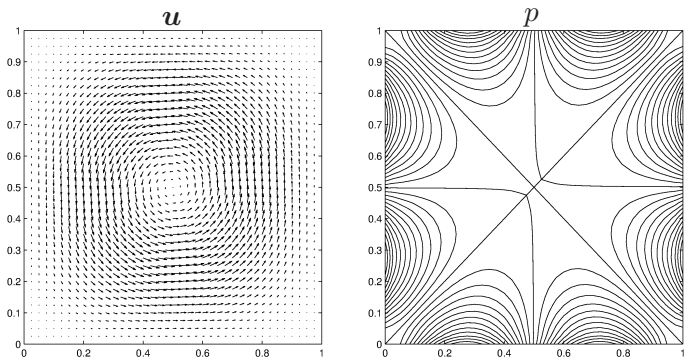

Figure 4: Plots of $\boldsymbol{u}$ and p for $N = 40$ with P_1 elements (two-field, square domain).

Table 6: Computed ten eigenvalues of two-field Stokes problem on a square domain using P_2 elements.

Ref.	$N = 10$	$N = 15$	$N = 20$	$N = 25$	$N = 30$	$N = 35$	$N = 40$
52.3447	52.3892	52.3542	52.3478	52.3460	52.3453	52.3450	52.3449
92.1245	92.2650	92.1540	92.1341	92.1285	92.1264	92.1255	92.1250
92.1246	92.3546	92.1731	92.1402	92.1310	92.1276	92.1261	92.1254
128.2100	128.8179	128.3406	128.2526	128.2276	128.2184	128.2144	128.2124
154.1260	154.7857	154.2660	154.1712	154.1445	154.1347	154.1305	154.1284
167.0298	167.8012	167.1932	167.0829	167.0516	167.0401	167.0351	167.0327
189.5729	190.8794	189.8582	189.6665	189.6116	189.5913	189.5825	189.5781
189.5735	191.5500	190.0079	189.7160	189.6322	189.6013	189.5879	189.5813
246.3240	248.3017	246.7483	246.4620	246.3806	246.3507	246.3377	246.3314
246.3243	248.6870	246.8347	246.4907	246.3926	246.3566	246.3409	246.3332

Table 7: Computed ten eigenvalues of three-field Stokes problem on a square domain using P_1 elements.

Ref.	$N = 10$	$N = 15$	$N = 20$	$N = 25$	$N = 30$	$N = 35$	$N = 40$
52.3447	56.5919	54.3902	53.5378	53.1231	52.8913	52.7491	52.6558
92.1245	98.9870	95.8558	94.4066	93.6468	93.2066	92.9310	92.7479
92.1246	106.0693	98.9834	96.1631	94.7706	93.9869	93.5043	93.1867
128.2100	148.9444	140.1753	135.6434	133.2037	131.7734	130.8721	130.2706
154.1260	172.7031	164.8846	160.9287	158.7355	157.4291	156.5992	156.0429
167.0298	189.4507	179.0202	174.4194	171.9815	170.5594	169.6654	169.0694
189.5729	212.7258	205.2605	199.9178	196.7485	194.7888	193.5145	192.6472
189.5735	238.4948	218.2487	207.5491	201.7170	198.2669	196.0809	194.6171
246.3240	269.6729	263.5867	258.3683	254.8240	252.5404	251.0333	250.0011
246.3243	282.5791	268.1758	260.8985	256.4580	253.6864	251.8820	250.6549

$N = 60$ using P_1 elements in Figure 4 for the two-field case, and in Figure 5 for the three-field case. Comparing these two figures, one can see the perfect agreement in the velocity and pressure profiles obtained with the two formulations. Moreover, we can observe that the behavior of the velocity streamlines and pressure levels are in good agreement with the previously published results [2, 20].

Before proceeding, we want to report an unexpected behavior we have encountered during our numerical experiments. As the numerical analysis for both two-field and three-field source problems suggests, the numerical constants in the stabilization parameters can be arbitrarily chosen in a wide range. Considering the source problems, for all cases this conclusion has been validated by testing different combinations of the parameters chosen from a very large interval. For

Table 8: Computed ten eigenvalues of three-field Stokes problem on a square domain using P_2 elements.

Ref.	$N = 10$	$N = 15$	$N = 20$	$N = 25$	$N = 30$	$N = 35$
52.3447	52.4156	52.3591	52.3493	52.3466	52.3456	52.3452
92.1245	92.2684	92.1548	92.1343	92.1285	92.1264	92.1255
92.1246	92.4690	92.1927	92.1461	92.1333	92.1287	92.1267
128.2100	129.306	128.4260	128.2782	128.2378	128.2232	128.2170
154.1260	154.6511	154.2415	154.1636	154.1414	154.1332	154.1297
167.0298	167.5411	167.1493	167.0696	167.0462	167.0375	167.0337
189.5729	191.4011	189.9504	189.6936	189.6223	189.5964	189.5852
189.5735	193.3702	190.3109	189.8036	189.6665	189.6175	189.5965
246.3240	246.4209	246.4648	246.3805	246.3486	246.3356	246.3297
246.3243	246.8890	246.5649	246.4125	246.3617	246.3419	246.3331

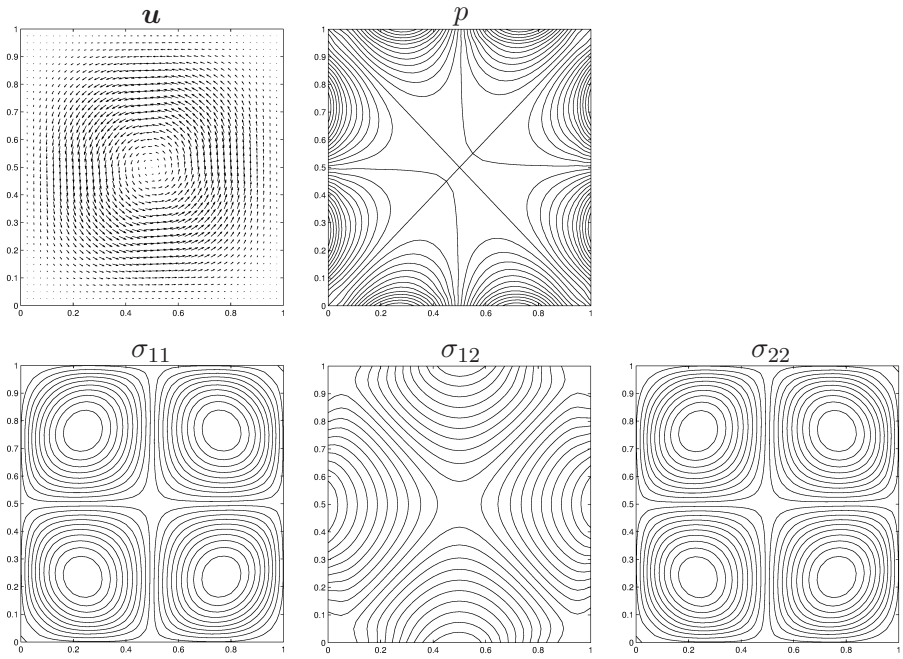

Figure 5: Plots of $\boldsymbol{u}$, p and $\boldsymbol{\sigma}$-components for $N = 40$ with P_1 elements (three-field, square domain).

the eigenvalue problems, this is also true for the two-field case. However, considering the approximation of first ten eigenvalues for the three-field eigenproblem, when we test the method with constants approximately ten times larger than our default values, we have observed that for certain cases spurious node-to-node os-

cillations in the approximations are developed. This bad behavior only exists in the seventh and tenth modes, and only for the three-field case for both P_1 and P_2 elements, using high values for the algorithmic constants. In other words, the correct values are well approximated for larger values of the stabilization constants for the two-field problem; however, a bad behavior is observed in two approximations of the first ten eigenvalues for the three-field case. These results lead us to think that a possible reason for this issue could be related to the deficiency of the algorithm that computes the eigenvalues for the structure of the resulting system in the three-field case.

5.2. Test 2: L-shaped domain

In the previous example we have considered a convex domain and showed that the convergence estimates are recovered numerically for both two-field and three-field cases. Next, we want to examine a test case with an L-shaped domain with a re-entrant corner, defined by $\Omega = [-1, 1]^2 \setminus [0, 1]^2$. The problem domain with a discretization where $N = 5$ is shown in Figure 6.

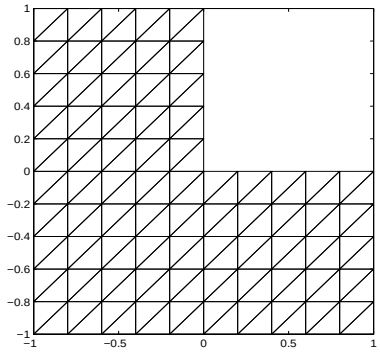

Figure 6: A sample triangulation of the L-shaped domain ($N = 5$).

For this experiment, we consider $\lambda_2 = 48.9844$ as the reference value to the fourth eigenvalue. It is known that the dual problem has $H^{\iota+1}$ regularity where $0 < \iota < 1$ [4]. The convergence results obtained for the two-field problem are shown in Figure 7, where the reference values are given in Table 9 and 10 using P_1 and P_2 elements, respectively. Similarly, Figure 8 plots the convergence results for the three-field case, whereas the approximated values are listed in Table 11 (P_1 results) and Table 12 (P_2 results). We conclude from these results that the method achieves a double order of convergence from above, for the errors of

the approximated eigenvalues. Further, we can infer that the reference eigenfunction corresponding to the fourth eigenvalue is smooth, complying with the results reported in [4].

Table 9: Computed eigenvalues of the two-field Stokes problem on a L-shaped domain using P_1 elements.

N	λ_h	$(\lambda_2 - \lambda_h)/\lambda_2$
5	58.6756	0.1978
10	51.8885	0.0593
15	50.3119	0.0271
20	49.7384	0.0154
25	49.4692	0.0099
30	49.3218	0.0069

Table 10: Computed eigenvalues of the two-field Stokes problem on a L-shaped domain using P_2 elements.

N	λ_h	$(\lambda_2 - \lambda_h)/\lambda_2$
5	49.8045	0.0167
10	49.0428	0.0012
15	48.9959	0.0002
20	48.9877	0.0001

5.3. Test 3: Cracked square domain

Having dealt with two examples having analytic solutions, we consider another domain with a re-entrant corner, namely, a square with a 45-degrees crack, as the last test. The problem domain is discretized by a sequence of unstructured triangular meshes, and the total number of vertices is denoted by M. Figure 9 shows the problem domain and a sample discretization where $M = 136$.

We take $\lambda_3 = 31.2444$ as the reference solution to the first eigenvalue for this experiment. The corresponding solution is known to be singular [4].

Table 11: Computed eigenvalues of the three-field Stokes problem on a L-shaped domain using P_1 elements.

N	λ_h	$(\lambda_2 - \lambda_h)/\lambda_2$
5	51.9184	0.0599
10	49.8498	0.0177
15	49.4469	0.0094
20	49.2607	0.0056
25	49.1658	0.0037
30	49.1120	0.0026

Table 12: Computed eigenvalues of the three-field Stokes problem on a L-shaped domain using P_2 elements.

N	λ_h	$(\lambda_2 - \lambda_h)/\lambda_2$
5	49.4628	0.0098
10	49.0224	0.0008
15	48.9923	0.0002
20	48.9867	0.0000

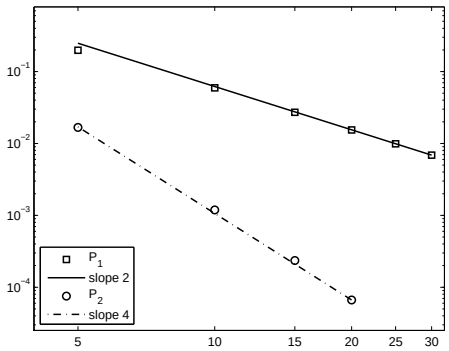

Figure 7: Plot of $\log|(\lambda_2 - \lambda_h)/\lambda_2|$ with respect to $\log|N|$ for the two-field Stokes problem on a L-shaped domain.

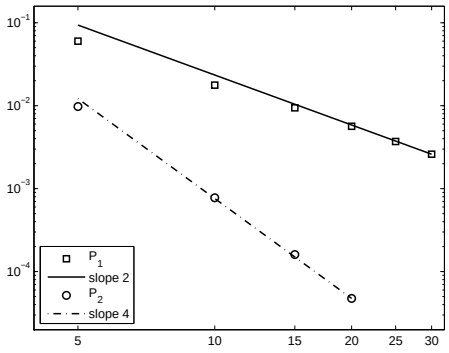

Figure 8: Plot of $\log|(\lambda_2 - \lambda_h)/\lambda_2|$ with respect to $\log|N|$ for the three-field Stokes problem on a L-shaped domain.

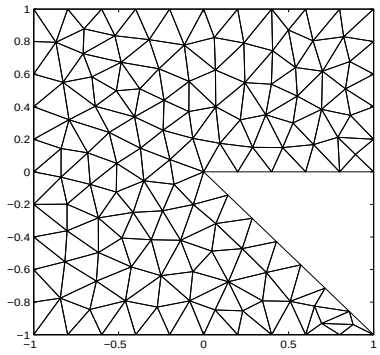

Figure 9: A sample triangulation of the cracked square ($M = 136$).

Tables 13 and 14 list the first eigenvalue approximations together with the relative errors, using P_1 and P_2 elements, respectively, for the two-field case. Similarly, in Tables 15 and 16 we present the results for the three-field case.

The convergence results in terms of the errors are displayed in Figure 10 for the two-field case and in Figure 11 for the three-field case. The results show that the monotonic approximation property of the method is also preserved for this example, and the approximation orders are higher than the reference value for all cases considered. The figures indicate that the asymptotic regime has not been reached yet, and the number of elements has to be further increased in order to obtain a linear dependence of the error on the number of total vertices. We clearly

Table 13: Computed eigenvalues of the two-field Stokes problem on a cracked square using P_1 elements.

M	λ_h	$(\lambda_3 - \lambda_h)/\lambda_3$
136	33.9006	0.0850
477	32.1248	0.0282
989	31.6912	0.0143
1861	31.4876	0.0078
2515	31.4485	0.0065
3489	31.4013	0.0050

Table 14: Computed eigenvalues of the two-field Stokes problem on a cracked square using P_2 elements.

M	λ_h	$(\lambda_3 - \lambda_h)/\lambda_3$
136	31.4697	0.0072
477	31.3694	0.0040
989	31.3215	0.0025
1861	31.3102	0.0021
2515	31.3074	0.0020
3489	31.3022	0.0018

infer that the convergence order has decreased for the problem where we do not have global regularity, and the solution is not analytic. Thus, we can conclude that the convergence is driven by the regularity of the continuous solution, as expected.

6. Conclusions

The stabilized finite element formulation based on the application of subgrid scale concept to the two-field and three-field Stokes eigenvalue problems has been presented. The virtue of the method relies in considering the subscales orthogonal to the finite element space; the fact that the orthogonal projection of the displacements (or velocities) vanishes provides an essential property which makes the method very convenient for eigenvalue problems. The finite element approxima-

Table 15: Computed eigenvalues of the three-field Stokes problem on a cracked square using P_1 elements.

M	λ_h	$(\lambda_3 - \lambda_h)/\lambda_3$
136	35.5336	0.1373
477	33.6856	0.0781
989	32.6086	0.0437
1861	32.0648	0.0263
2515	31.9739	0.0233
3489	31.8046	0.0179

Table 16: Computed eigenvalues of the three-field Stokes problem on a cracked square using P_2 elements.

M	λ_h	$(\lambda_3 - \lambda_h)/\lambda_3$
136	32.0113	0.0245
477	31.6124	0.0118
989	31.4632	0.0070
1861	31.4086	0.0053

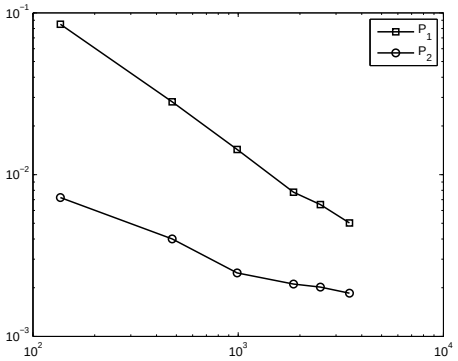

Figure 10: Plot of $\log|(\lambda_3 - \lambda_h)/\lambda_3|$ with respect to $\log|M|$for the two-field Stokes problem on a cracked square domain.

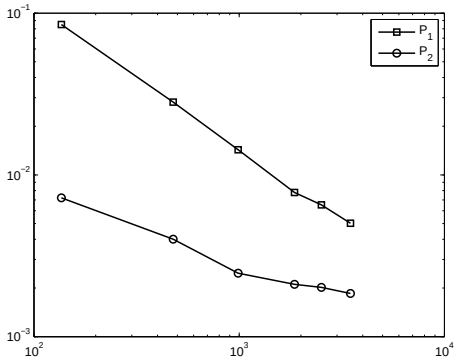

Figure 11: Plot of $\log|(\lambda_3 - \lambda_h)/\lambda_3|$ with respect to $\log|M|$ for the three-field Stokes problem on a cracked square domain.

tion to the three-field Stokes eigenvalue problem is another novel contribution of the paper. The convergence and error estimates are based on the finite element analysis of the corresponding source problems. The formulations are shown to be optimally convergent for a given set of algorithmic parameters on which the methods depend. The numerical computations show that the accuracy of the method is the one expected from the convergence analysis, and the theoretical convergence rates for all the experiments considered are exactly achieved in the numerical results presented.

Acknowledgments

The first author acknowledges the support received from the Scientific and Technological Research Council of Turkey (TUBITAK) 2219-Postdoctoral Research Program Grant. The second author was partially supported by PRIN/MIUR, by GNCS/INDAM, and by IMATI/CNR. The third author is grateful to the ICREA Acadèmia Program, from the Catalan government.

References

[1] B. Mercier, J. Osborn, J. Rappaz, and P.-A. Raviart, "Eigenvalue approximation by mixed and hybrid methods," *Math. Comp.*, vol. 36, no. 154, pp. 427–453, 1981.

[2] M. G. Armentano and V. Moreno, "A posteriori error estimates of stabilized low-order mixed finite elements for the Stokes eigenvalue problem," *Journal*

of Computational and Applied Mathematics, vol. 269, no. 0, pp. 132 – 149, 2014.

[3] P.-z. Huang, Y.-n. He, and X.-l. Feng, "Two-level stabilized finite element method for Stokes eigenvalue problem," *Applied Mathematics and Mechanics*, vol. 33, no. 5, pp. 621–630, 2012.

[4] H. Liu, W. Gong, S. Wang, and N. Yan, "Superconvergence and a posteriori error estimates for the Stokes eigenvalue problems," *BIT Numerical Mathematics*, vol. 53, no. 3, pp. 665–687, 2013.

[5] H. Xie and X. Yin, "Acceleration of stabilized finite element discretizations for the Stokes eigenvalue problem," *Advances in Computational Mathematics*, pp. 1–14, 2014.

[6] P. Huang, "Lower and upper bounds of Stokes eigenvalue problem based on stabilized finite element methods," *Calcolo*, vol. 52, no. 1, pp. 109–121, 2015.

[7] S. Meddahi, D. Mora, and R. Rodrguez, "A finite element analysis of a pseudostress formulation for the Stokes eigenvalue problem," *IMA Journal of Numerical Analysis*, 2014.

[8] I. Babuška and J. Osborn, "Eigenvalue problems," in *Finite Element Methods (Part 1)*, vol. 2 of *Handbook of Numerical Analysis*, pp. 641 – 787, Elsevier, 1991.

[9] D. Boffi, "Finite element approximation of eigenvalue problems," *Acta Numerica*, vol. 19, pp. 1–120, 5 2010.

[10] D. Boffi, F. Brezzi, and L. Gastaldi, "On the convergence of eigenvalues for mixed formulations," *Ann. Scuola Norm. Sup. Pisa Cl. Sci. (4)*, vol. 25, no. 1-2, pp. 131–154 (1998), 1997. Dedicated to Ennio De Giorgi.

[11] R. Codina, "Finite element approximation of the three field formulation of the Stokes problem using arbitrary interpolations," *SIAM Journal on Numerical Analysis*, vol. 47, pp. 699–718, 2009.

[12] J. Bonvin, M. Picasso, and R. Stenberg, "GLS and EVSS methods for a three fields Stokes problems arising from viscoelastic flows," *Computer Methods in Applied Mechanics and Engineering*, vol. 190, pp. 3893–3914, 2001.

[13] R. Codina, "Analysis of a stabilized finite element approximation of the Oseen equations using orthogonal subscales," *Applied Numerical Mathematics*, vol. 58, pp. 264–283, 2008.

[14] R. Codina and J. Blasco, "A finite element formulation for the Stokes problem allowing equal velocity-pressure interpolation," *Computer Methods in Applied Mechanics and Engineering*, vol. 143, pp. 373–391, 1997.

[15] V. Girault and P. Raviart, *Finite element methods for Navier-Stokes equations*. Springer–Verlag, 1986.

[16] R. Codina, "Stabilization of incompressibility and convection through orthogonal sub-scales in finite element methods," *Computer Methods in Applied Mechanics and Engineering*, vol. 190, pp. 1579–1599, 2000.

[17] R. Codina, "On stabilized finite element methods for linear systems of convection-diffusion-reaction equations," *Computer Methods in Applied Mechanics and Engineering*, vol. 188, pp. 61–82, 2000.

[18] D. Boffi, F. Brezzi, and L. Gastaldi, "On the problem of spurious eigenvalues in the approximation of linear elliptic problems in mixed form," *Math. Comp.*, vol. 69, no. 229, pp. 121–140, 2000.

[19] M. Fortin and R. Pierre, "On the convergence of the mixed method of crochet and marchal for viscoelastic flows," *Computer Methods in Applied Mechanics and Engineering*, vol. 73, pp. 341–350, 1989.

[20] P. Huang, Y. He, and X. Feng, "Numerical investigations on several stabilized finite element methods for the Stokes eigenvalue problem," *Mathematical Problems in Engineering*, vol. 2011, no. 745908, pp. 1–14, 2011.